Journal of Structural Geology, Vol. 13, No. 9, pp. 1025 to 1035, 1991
Printed in Great Britain

0191-8141/91 $03.00 + 0.00

Displacements and segment linkage in strike-slip fault zones

D. C. P. PEACOCK

Department of Geology, University of Southampton, Southampton SO9 5NH, U.K.

(*Received 29 November 1990, accepted in revised form 27 March 1991*)

Abstract—Small scale, well exposed strike slip fault zones near Kirkcudbright, Scotland, cut sub vertical bedding, so that mapped bed separations allow the displacements, linkage and evolution of fault segments to be assessed. Displacement variations along the segments can be related to lithologic variations, conjugate relationships, offsets, segment linkage and fault bends. High displacement gradients at the tips of conjugate and offset faults produce convex upwards (*E type*) displacement–distance (d–x) profiles. Contractional fault bends and linkage points are marked by a decrease in fault displacement, producing partially concave upwards (*D type*) d–x profiles. Where fault displacement gradients are steep, wallrocks are marked by structures such as synthetic faults, normal drag folding, ductile strain and veining, which transfer displacement. The faults studied tend to have lower r/d_{MAX} ratios (where r = distance between the point of maximum displacement and the fault tip on a particular profile, and d_{MAX} = maximum displacement on the profile) than are shown by normal faults in map view. This may be because r is measured parallel to the displacement direction and/or because of lithologic variations.

INTRODUCTION

STRIKE SLIP fault zones usually consist of complex patterns of segments, each adding to the displacement of the zones. This is clear from maps of strike slip fault zones (e.g. Wilcox *et al.* 1973) and from the study of the seismicity of fault zones (e.g. King 1983, 1986). Knowledge of the displacement characteristics of fault segments is thus important in understanding the overall development of fault zones. This paper describes displacement variations along strike slip fault segments, and interprets the variations in terms of the effects on fault development of lithologic variations, conjugate relationships, offsets, segment linkage, and bends. Five small-scale strike slip fault zones are described from Silurian sandstone–shale sequences at Raeberry (grid reference NX699437) and Gipsy Point (grid reference NX685435), near Kirkcudbright, Scotland (Fig. 1).

The map views of strike slip faults at Raeberry and Gipsy Point show displacement parallel and bedding normal profiles. These can be compared with the displacement normal and bedding parallel profiles of normal faults in map view described by Peacock & Sanderson (1991). Differences between the two groups of faults can be related to their relationships between displacement direction and bedding anisotropy. The strike slip faults described here are probably very similar to vertical cross sections through normal faults.

GENERAL DESCRIPTION OF THE FAULT ZONES

The fault zones at Raeberry and Gipsy Point show the segmentation which is typical of strike slip fault zones (e.g. Wilcox *et al.* 1973). The fault zones were mapped at a scale of approximately 1:25, using mosaics of aerial photographs taken using a camera at the top of a tripod and pole (total height 7.3 m). A rope with markers at 1 m

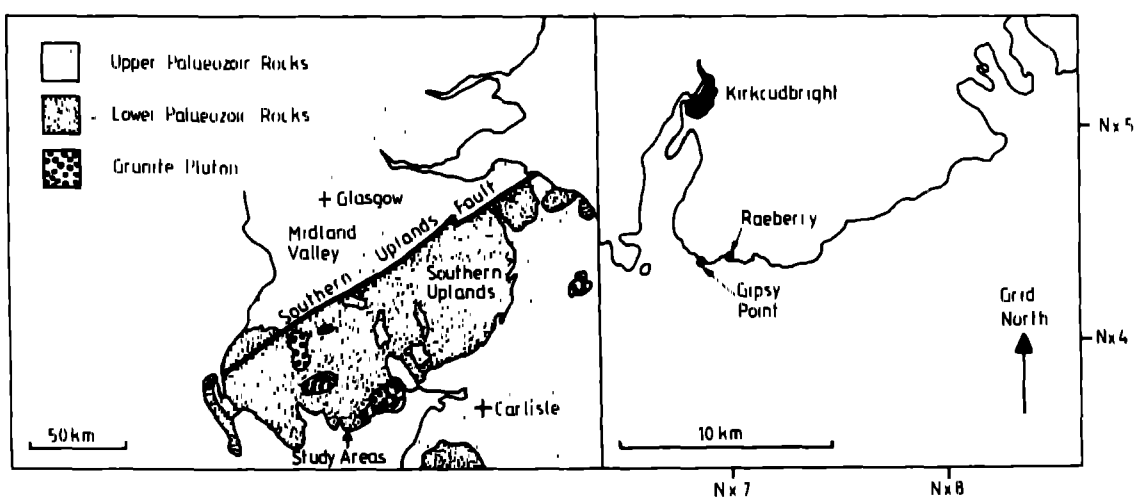

Fig. 1. Map of SW Scotland, showing the location of the field areas. Raeberry is at grid reference NX699437, and Gipsy Point is at NX685435.

intervals, placed along the length of the fault zones, aided linkage of the photographs Some distortions occur because of imperfect fit of the photographs and because of topographic variations These problems were reduced at Gipsy Point by using aerial photographs as templates (the aerial photographs were taken by J. Allen of St Andrews University, using a model aeroplane) Segments at Raeberry are designated by R, and those at Gipsy Point are designated by G, with the segments numbered Portions of segments north or south of the maximum displacement are denoted by (N) or (S), respectively For instance, the southern end of segment 8 at Raeberry may be termed R8(S)

The two study areas are in the lower Palaeozoic (Caledonian) Southern Uplands-Longford Down Terrane As outlined by McKerrow (1987), this terrane has been interpreted as an accretionary wedge (McKerrow *et al.* 1977, Leggett *et al.* 1979, Kemp 1986, Needham & Knipe 1986, Leggett 1987, McCurry & Anderson 1989), or as a back arc/successor basin (Murphy & Hutton 1986, Hutton & Murphy 1987, Stone *et al* 1987, Barnes *et al* 1989) The strike slip faults described here were produced by approximately N-S directed compression, which post dates the strike parallel contractional faults Both areas consist of Silurian sandstone and shale turbidites, in beds up to 3 m thick (Kemp 1986).

STRUCTURES AT RAEBERRY AND GIPSY POINT

This paper is concerned with strike-slip faults at high angles to bedding which occur at Raeberry and Gipsy Point. They have strike slip displacements of up to at least 5 m, measured using displaced beds, although the fault zones described here have displacements of up to 1 m. Fault planes are well exposed and are often marked by calcite or dolomite. Fault, vein and bed dip data are shown in Fig. 2. It is assumed that veins are normal to σ_1 (fibres are dominantly normal to vein walls), that slickensides are normal to σ_2, and that sinistral and dextral faults intersect at σ_3 The faults often show fault tip folds with extensional kink band geometries, with up to approximately 50 mm displacement (Fig. 3) Where sandstone beds are folded, braided fractures occur which are similar to those shown by Engelder (1987, fig 2.9) The fault tip folds are preserved as apparent normal drag where the fault has propagated through them Rhomb shaped pull aparts develop where faults cut sandstones at a high angle, and are refracted at a lower angle through the shales (Peacock & Sanderson 1991, fig 4) The pull aparts tend to reduce the angle between conjugate faults to about 30°

Folding occurs around Raeberry, but does not affect the fault zones studied, where bedding is sub vertical (±10°) and strikes at about 055° (Fig. 2a). At Gipsy Point, folds occur in slumped units (Kemp 1986), but elsewhere bedding dips consistently at about 79° to the north west (Fig 2b). Sub vertical contractional kink bands (Ramsay & Huber 1987, fig 20 28) occur at Gipsy Point, mostly in thick shale units These form conjugate

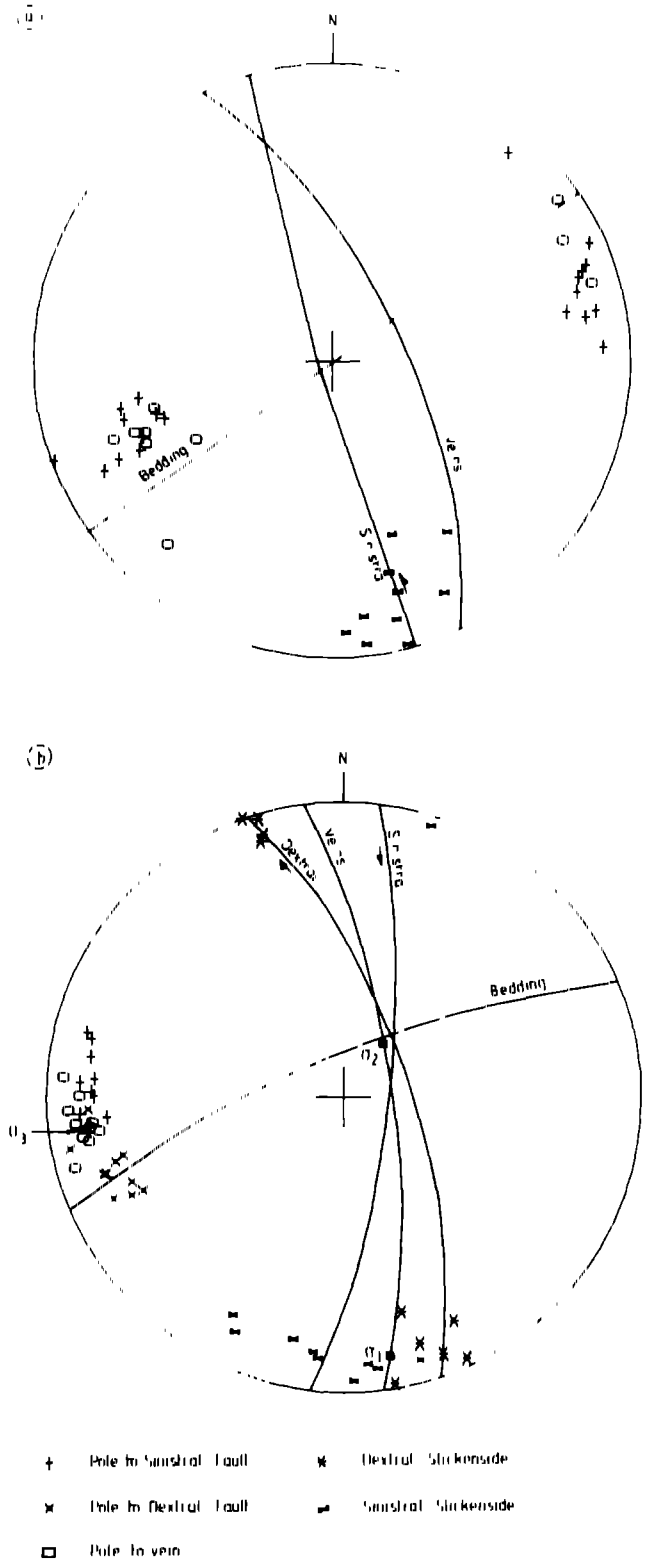

Fig 2 (a) Stereogram of Raeberry data (b) Stereogram of Gipsy Point data

sets striking at about 003° (dextral) and 120° (sinistral), and are occasionally cut by strike slip faults

At Gipsy Point, one group of faults at a low angle to bedding are displaced by, and so pre date, the strike slip faults These may be related to the unit bounding contractional fault zones described by Kemp (1987) The displacement direction is not clear, but a fault in the

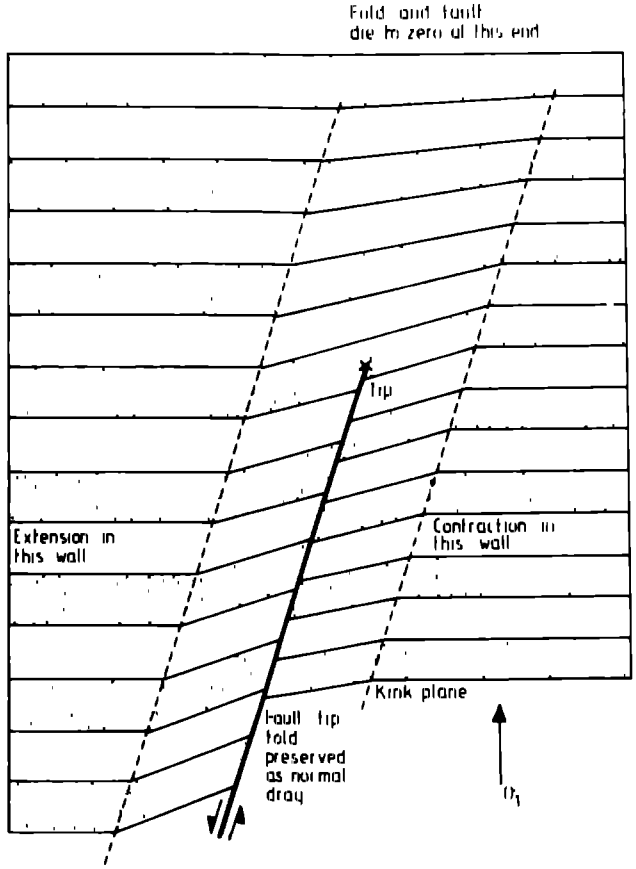

Fig. 3. Diagram of extensional kink band type folding at a fault tip, this being preserved as apparent drag along the propagating fault. At Gipsy Point, the folds have displacements of about 50 mm. Relative extension and contraction occur in the wallrocks on either side of the fault. Stippled and unstippled layers represent bedding, but do not have lithological significance.

north west of the area shows drag which indicates sinistral shear. Another group of faults at a low-angle to bedding tend to cut the strike slip faults; two such fault zones occur in the north and south of the mapped fault zones, with evidence of duplex development in the northern zone. These low angle faults appear to be anisotropy controlled reverse faults, possibly developed at a high angle to σ_1 in the same N-S directed compressional stress system as the strike slip faults.

DISPLACEMENTS ALONG STRIKE-SLIP FAULT SEGMENTS

The displacement–distance (d-x) method (Williams & Chapman 1983) is used to analyse the faults, with offset beds marking strike slip displacements. Distance is measured in a straight line from the northern end of each segment, as an approximation for the actual distance along the trace. Displacements for small synthetic branches are added to the main fault, with larger segments being measured separately. Normal drag has been measured, but is not included on the d-x graphs. Ductile wallrock deformation tends to smooth out d-x profiles when it is added to fault displacement (Walsh & Watterson 1987). Normalized displacement–distance data (D-X graphs, see Peacock & Sanderson 1991) for the

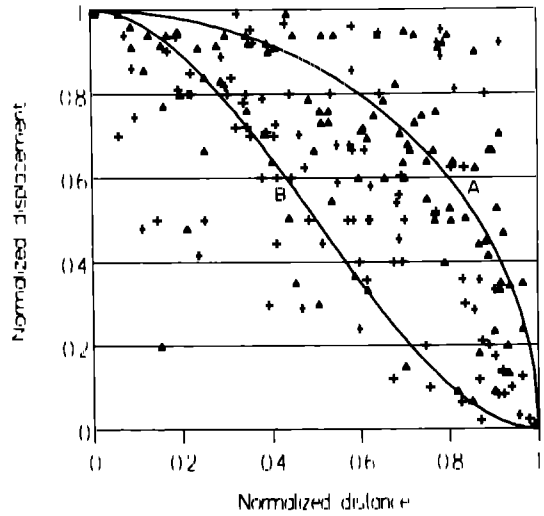

Fig. 4. Normalized displacement–distance (D-X) data for segments at Raeberry (triangles) and Gipsy Point (crosses), consisting of 285 data points from 30 segments. Profiles for the single event elastic model (A) and the Walsh & Watterson (1987) cumulative slip model (B) are also shown.

strike slip faults at Raeberry and Gipsy Point (Fig. 4) show considerable scatter. Variability in D-X data is explained here in terms of fault displacement variations caused by lithologic variations, conjugate relationships, offsets, segment linkage and fault bends.

Classification of displacement–distance profile types

Several d-x profile types have been described (Fig. 5) (see Peacock & Sanderson 1991). Pollard & Segall (1987) described single-event ideal elastic fractures, with elliptical d-x profiles (here termed *ideal* or *I-type*). Walsh & Watterson (1987) derived a *cumulative slip* profile for isolated planar faults by assuming that propagating faults accumulate slip increments according to the elastic model, the amount of incremental slip being proportional to fault length. The cumulative-slip profile

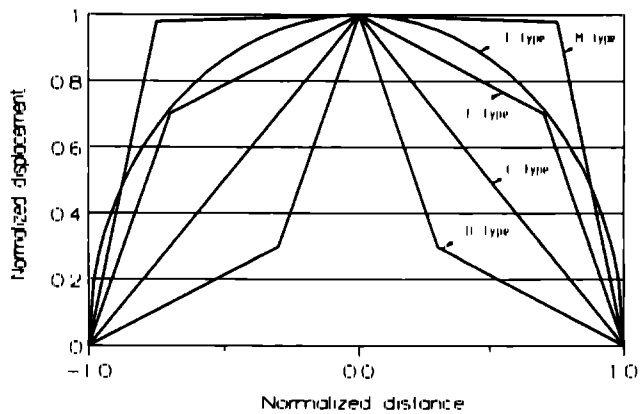

Fig. 5. Idealized displacement–distance (d-x) graph, showing a classification of d-x profiles. The graph is normalized (i.e. D-X), with the point of maximum displacement at distance zero and the tips at −1 and 1. This is done to illustrate the relationship between normalized and non normalized data. I type = ideal elastic, C type = cone shaped, M type = mesa shaped, E type = *elevated* above the C type profile; D type = *depressed* below the C type profile. E types can be similar to I types, but are not gently curved. See text for explanation.

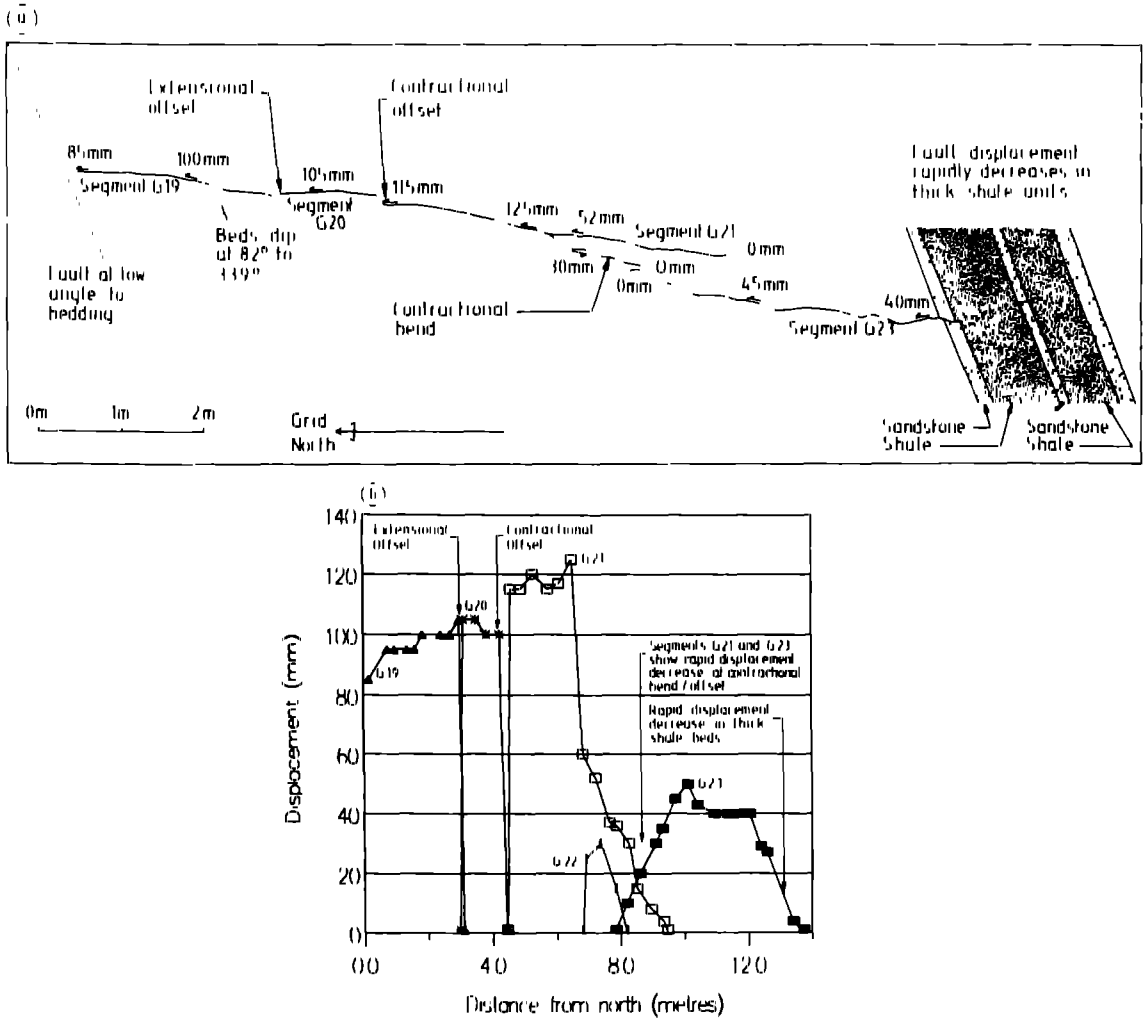

Fig. 6. (a) Simplified map of a fault zone at Gipsy Point. Two thick shale units are shown in the south of the zone. The rest of the sequence consists of shale and sandstone beds averaging about 0.2 m wide. (b) Displacement–distance (d–x) graph for (a). Displacement on segment G23 decreases rapidly southwards in the thick shale units, this producing an E type D–X graph for the south of G23. Displacement also decreases rapidly southwards at the contractional bend, producing a D type profile for the south of the whole fault zone.

approximates to the *C type* (cone-shaped) profile described by Muraoka & Kamata (1983), which is typical of faults in homogeneous incompetent material. Muraoka & Kamata (1983) also described *M-type* (mesa shaped) profiles which have a flat central portion where they cut a rigid unit, and steep flanks with high displacement gradients where they pass into incompetent units.

Faults usually differ from the cumulative-slip profile because of complexities in their slip-propagation relationships. Two more d–x profiles can be defined (Fig. 5) from the data of Peacock & Sanderson (1991) and from the Raeberry and Gipsy Point data. Firstly, *E type* profiles, which are partially or completely *elevated* above the C-type profile, and are convex upwards. These occur where steep displacement gradients are developed at fault tips. Secondly, *D type* profiles, which are partially or completely *depressed* below the C type profile, and are partially concave upwards.

This five fold classification of d–x profiles (Fig. 5) is complex, and it may be difficult to assign fault data to an individual class. E type profiles can be similar to I-types, but are not gently curved. The generic term I-type should not be used unless it is certain that the profile is of a single event fracture. The term M type, as used by Muraoka & Kamata (1983), also has generic implications, and should be applied only to profiles with flat portions around the point of maximum displacement.

Effects of lithologic variations

Muraoka & Kamata (1983) discussed the effects of lithologic variations on d–x profiles, and showed that competent units can either initiate or inhibit faulting, depending on whether stress concentration in competent units exceeds their strength. At Raeberry and Gipsy Point, faults tend to cut several units, so the effects of lithologic variations are difficult to distinguish. However, displacement on fault G23 appears to decrease rapidly southwards in thick shale units (Fig. 6). Fault R21 (Fig. 7) appears to have been unable to propagate through a thick sandstone unit southwards. E-type profiles are produced because propagation is hindered but displacement continues to accumulate, causing a steep displacement gradient at the fault tip.

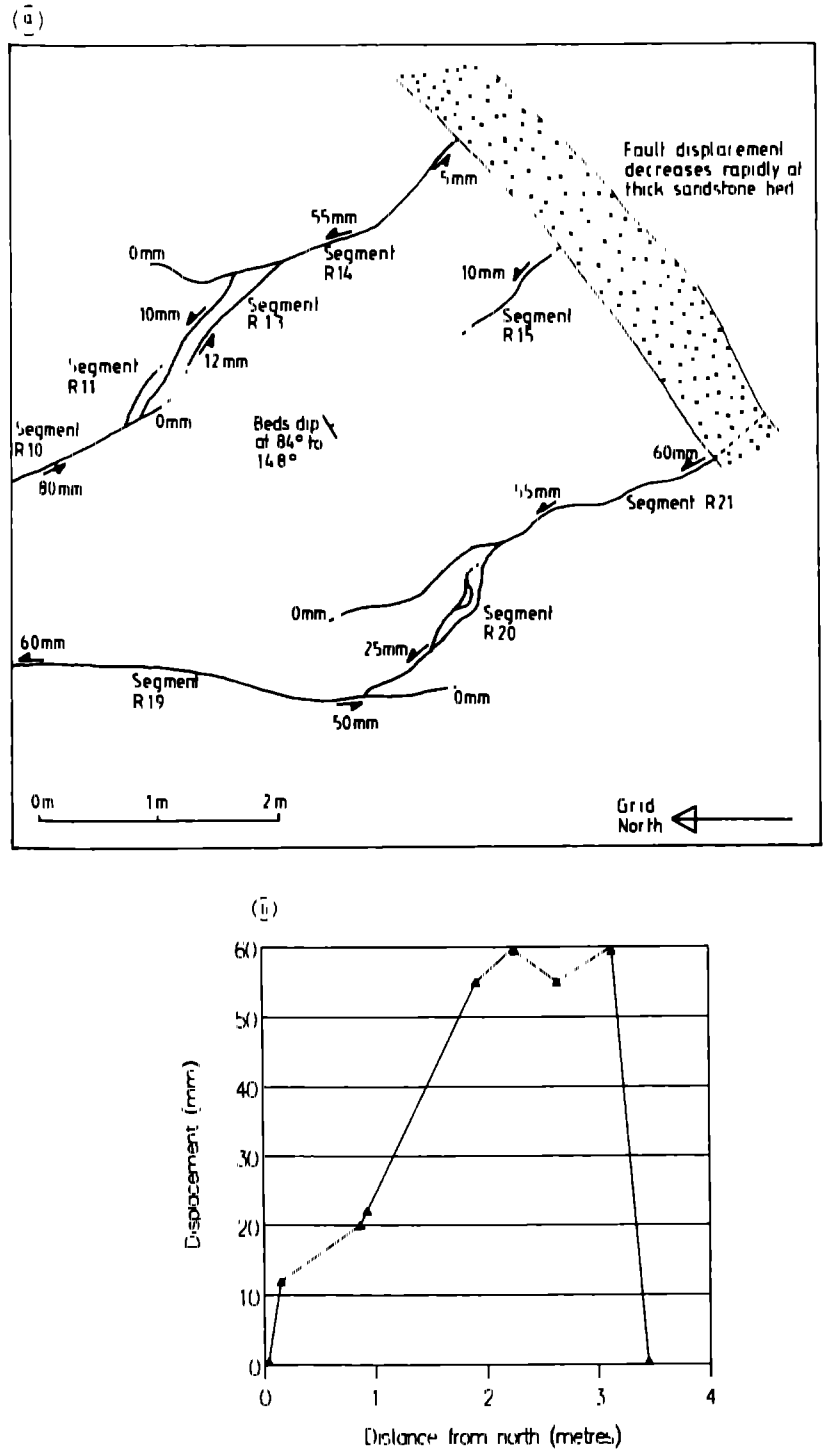

Fig. 7 (a) Simplified map of a fault zone at Raeberry (b) Displacement–distance graph for segment R21 in (a), which has a steep displacement gradient southwards apparently caused by an inability of the faults to propagate through the thick sandstone bed

Conjugate relationships

Conjugate segments G25 and G28 show E-type d–x profiles (Fig. 8). It appears that propagation and slip are inhibited by interaction between the faults (Fig. 9). The point of maximum displacement can probably migrate away from the point of fault initiation. Horsfield (1980) demonstrated that conjugate normal faults can show systematic cross-cutting relationships. This study shows that it is not necessary for conjugate faults to cross cut; instead they can meet at a point of zero displacement, around which strain builds up until new conjugate systems develop away from the initial meeting point

Offset segments

Walsh & Watterson (1987) demonstrate that isolated normal faults have approximate C-type profiles, and Peacock & Sanderson (1991) establish that an E type profile is produced as interaction occurs between offset normal faults. Contractional and extensional offsets along strike slip faults at Raeberry and Gipsy Point

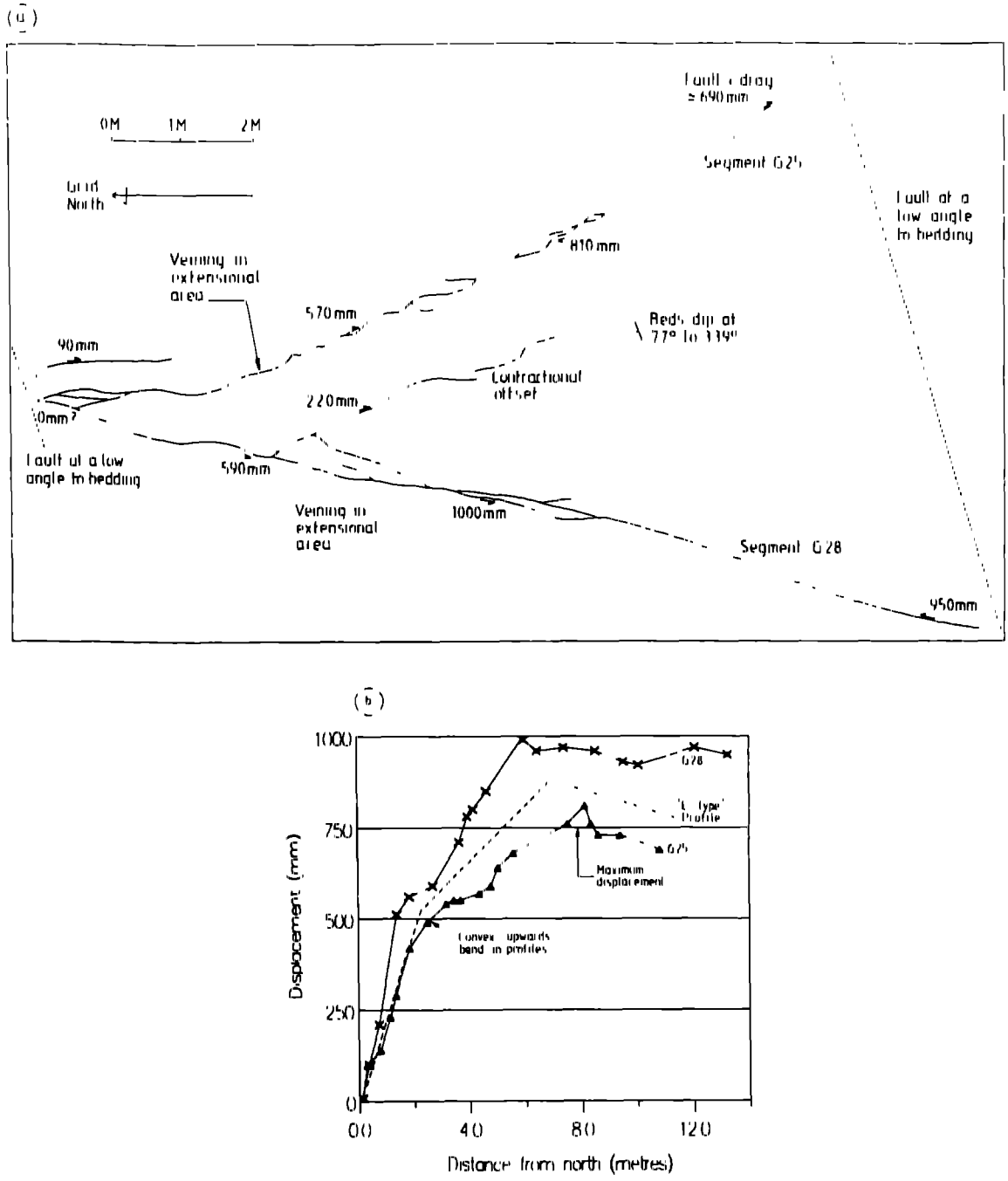

Fig. 8. (a) Simplified map of conjugate faults at Gipsy Point. (b) Displacement–distance graph for segments G25 and G28 in (a). The conjugate segments have steep displacement gradients where they interact and join (northwards), and thus have E type d–x graphs. An idealized E type profile is shown on the graph. The steep displacement gradient appears to be partially accommodated by considerable veining in the extensional areas of the wallrocks.

(Figs. 10 and 11) also show the development of E type d–x profiles, as interaction produces high displacement gradients at offset tips. Contractional offsets are concentrated in shales (Fig. 10), where high displacement gradients are accommodated (Muraoka & Kamata 1983). Small extensional offsets can occur in the competent sandstones, where they can form calcite-dolomite rhomb-shaped pull aparts (Fig. 11). There appears to be little difficulty in creating extensional openings in the sandstones, where pull-aparts are developed because of fault refraction. Displacements can be rapidly transferred by single beds when the offset and displacements are of the same order of magnitude as the bed thickness. When the offset is larger (e.g. Fig. 7a), displacement is transferred more gradually, often by veining and connecting faults.

Linkage of initially offset segments

Initially offset segments can be linked by connecting faults to eventually form contractional or extensional bends. Linkage points are usually marked by displacement minima, which may produce D type profiles (Fig. 12) (Peacock & Sanderson 1991). Structures between segments G21 and G23 (Figs. 6 and 12) represent an example of a contractional linkage, and structures be

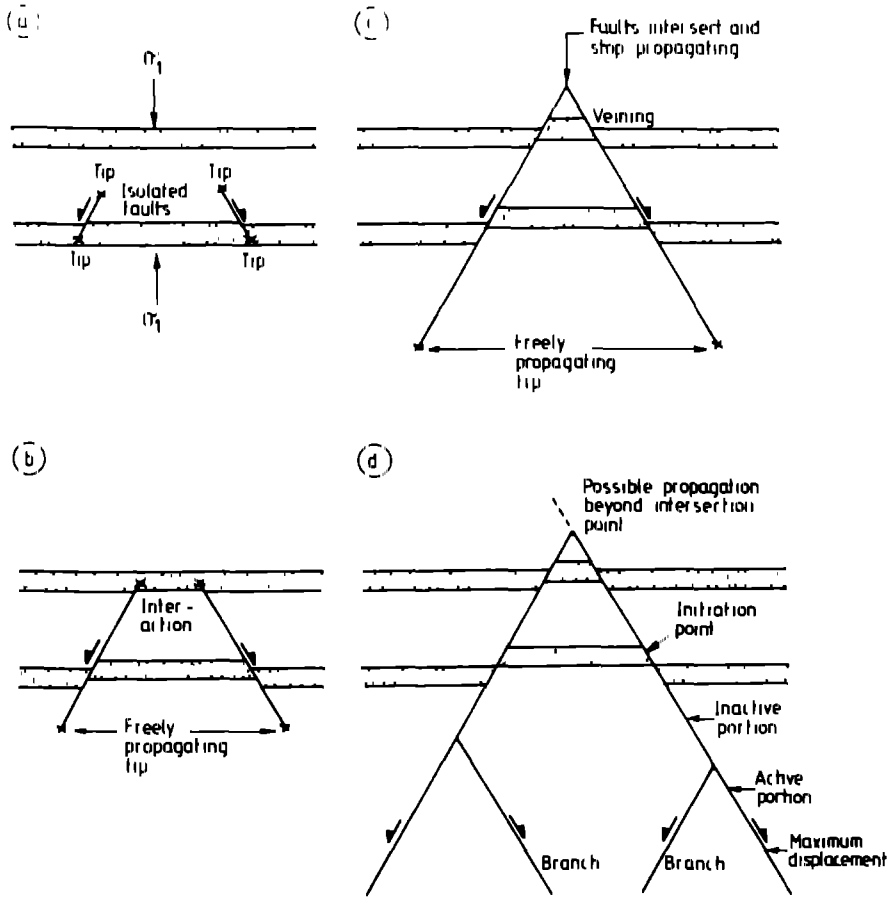

Fig. 9. Possible stages in the development of conjugate systems. (a) Initially isolated, non interacting faults. (b) Interaction starts to occur. (c) The fault tips meet and further propagation is halted, with high displacement gradients partly accommodated by veining near the intersection. (d) Further displacement occurs by the development of new conjugate systems, or by one of the faults propagating beyond the intersection point.

tween segments R10 and R14 (Figs. 7a and 12) represent an example of an extensional linkage. Fault displacement minima at linkage points also occur on linked normal faults (Peacock & Sanderson 1991) where destroyed relay ramps are preserved as normal drag. Ellis & Dunlap (1988) describe displacement minima at thrust linkage points.

From the above, four stages can be recognized in the development of displacement parallel offsets at Raeberry and Gipsy Point (Fig. 13).

(a) Initial development of non overlapping faults, each with an approximately linear d–x profile.

(b) Overlap development as fault segments propagate towards each other, causing the displacement gradient to increase at offset tips. Displacement is transferred between the offset faults by ductile deformation or by minor fractures.

(c) Connecting fault(s) link the offset segments.

(d) The offset is destroyed, producing an extensional or contractional bend.

Fault bends

Fault bends can be produced by the linkage of offsets (Fig. 13), or by variations in the propagation direction of a single fault. Extensional and contractional bends show a decrease in fault displacement when they are formed from the linkage of two segments which each have maximum displacement away from the bend (Figs. 6, 7 and 12). After extensional bends form, they do not appear to cause further displacement variations because there is no tendency for volume decrease and normal drag. In contrast, contractional bends are characterised by displacement minima caused by normal drag, which accommodates the tendency for volume decrease at the bend (G19–G23 in Figs. 6 and 12). Ellis & Dunlap (1988) showed that fault bends usually represent barriers to displacement. It is probable that the displacement gradient will increase until the bend is broken down by synthetic (Woodcock & Fischer 1986, Swanson 1989, 1990) or antithetic faults.

Structures which transfer displacement at fault tips, offsets and bends

At Raeberry and Gipsy Point, displacement is transferred at fault tips, offsets and bends by synthetic faults, normal drag folding, ductile strain and veining. Synthetic faults transfer displacement between extensional and contractional offsets which are too large for displacement to be transferred by ductile strain in single shale units, an example being Fig. 7(a), where the offsets are much larger than bed thickness. Normal drag folding (Fig. 3) occurs at the tips of faults and at contractional

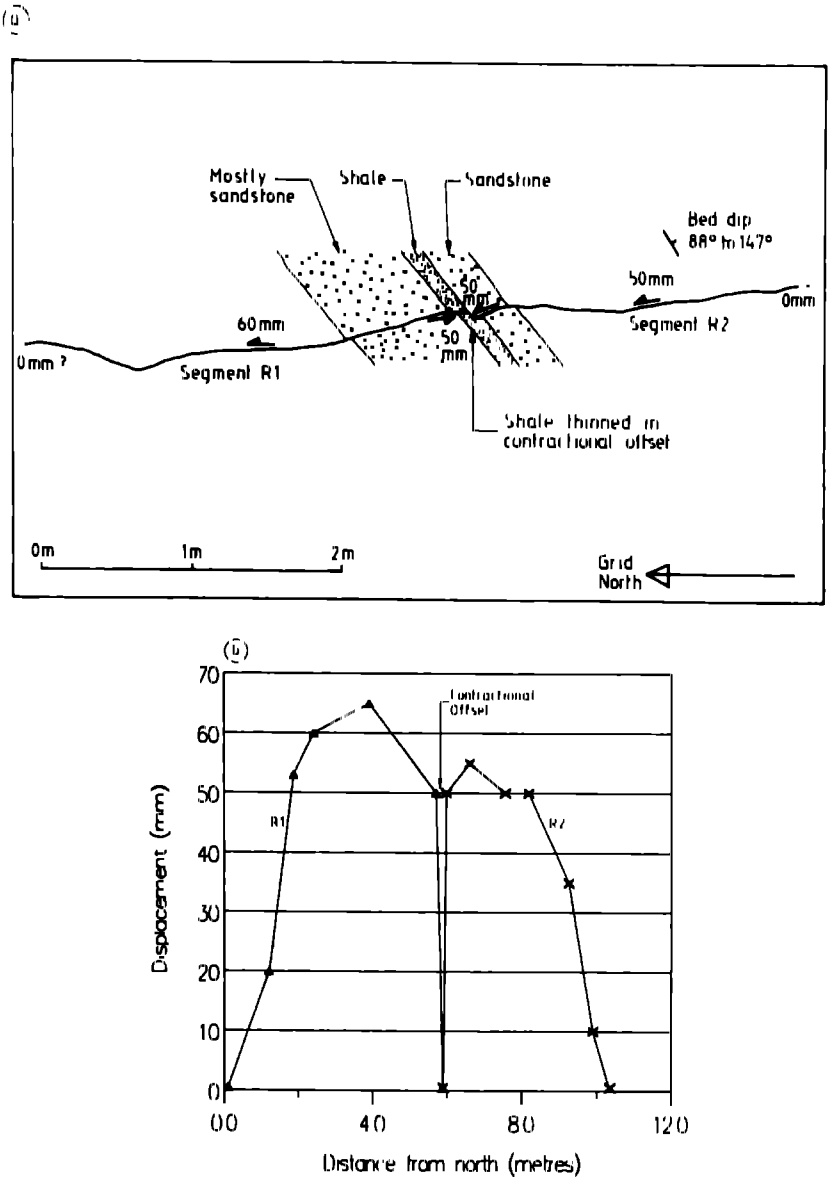

Fig. 10. (a) Simplified map of a fault zone with a contractional offset at Raeberry. (b) Displacement–distance graph for the faults in (a). The segments show steep displacement gradients at the offset. Displacement transfer at the offset is accommodated by thinning of the shale bed.

bends and offsets (Figs. 12 and 13). The shales can accommodate large amounts of ductile strain and high displacement gradients (Fig. 10). As shown in Fig. 3, the wallrocks on one side of a fault can show relative contraction, whilst those on the other side show relative extension. Veins are common in the extensional areas of wallrock (Fig. 8a), and are preferentially developed in the sandstones. Granier (1985, figs. 2a and 9d) showed this pattern of horsetail veining at offset and conjugate faults. It seems likely that horsetails (and other fault related structures) develop where there are high displacement gradients at fault tips, and develop to accommodate wallrock strain.

r/d_{MAX} RATIOS FOR RAEBERRY AND GIPSY POINT

Figure 14 shows a graph of r against d_{MAX} for the strike-slip fault segments at Raeberry and Gipsy Point (where r = distance between the point of maximum displacement and the fault tip on a particular profile, and d_{MAX} = maximum displacement on the profile). The faults are exposed parallel to the displacement direction, which is normal to anisotropy. The r/d_{MAX} values range from 1.34 to 109, which shows that the faults have considerable variability. The average r/d_{MAX} ratio of the segments is 24.2. These values can be compared with the average r/d_{MAX} ratio of 143 for isolated British coalfield normal faults (Walsh & Watterson 1987) and 65.3 for the normal fault segment data of Peacock & Sanderson (1991), which are exposed normal to the displacement direction. Although it is possible that the strike slip faults at Raeberry and Gipsy Point are geometrically and/or mechanically different from the coalfield faults and those of Peacock & Sanderson (1991), the lower values for Raeberry and Gipsy Point could be explained in terms of two related effects.

First, the relationship between the directions of displacement and lithologic variations may have an effect

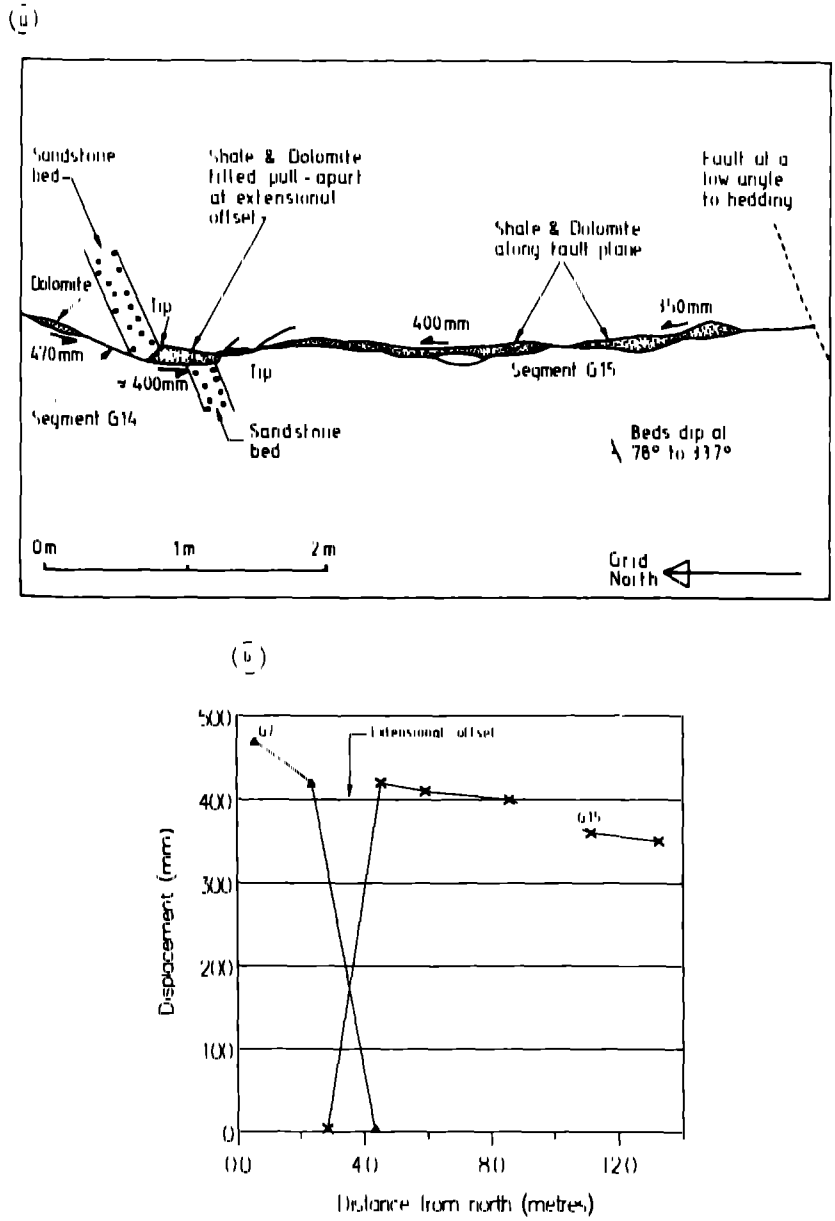

Fig 11 (a) Simplified map of a fault zone with an extensional offset at Gipsy Point Dolomite occurs as void mineralization in the pull aparts (rhombochasms), with injection of wallrock shales also occurring (b) Displacement–distance graph for the faults in (a) The segments show steep displacement gradients at the offset Displacement transfer at the offset is accommodated by a rhomb shaped pull apart, which is filled by dolomite and shale material

on elliptical fault shape Barnett *et al.* (1987) showed that isolated normal faults in sub horizontal bedding ideally have elliptical tip lines, with the long axis (direction of lowest displacement gradient) normal to the displacement direction. British coalfield faults (Walsh & Watterson 1987) and the normal faults of Peacock & Sanderson (1991) are therefore probably measured parallel to the long axis of fault ellipse Barnett *et al* suggest that the elliptical fault shape is caused by lithologic variations Such a pattern is indicated by the results of Muraoka & Kamata (1983), who show that the r/d_{MAX} ratios of C type faults tend to be nearly twice as large as those of M-types This is because the M-type profiles have very high displacement gradients in incompetent units at fault tips. The long axis of the fault ellipse will therefore be parallel to bedding, and it seems probable that strike-slip faults cutting sub-vertical bedding (as at Raeberry and Gipsy Point) will also have short axes parallel to the displacement direction The average r/d_{MAX} ratio for normal fault segments of Peacock and Sanderson (1991) (65.3) divided by the average r/d_{MAX} ratio for strike slip segments at Raeberry and Gipsy Point (24.2) is 2.7 This ratio is within the ellipticity values (1.25–3) for British coalfield normal faults found by Walsh & Watterson (1989)

Second, the slip and propagation variations caused by conjugates, offsets and bends can also explain the relatively low r/d_{MAX} ratios. Displacement parallel bends and offsets at Raeberry and Gipsy Point tend to have higher displacement gradients than the displacement normal bends and offsets described by Peacock & Sanderson (1991). This may be because displacement can be transferred more rapidly by the displacement normal anisotropy at Raeberry and Gipsy Point The minimum r/d_{MAX} ratio at Gipsy Point (1.34) is for segment G19(S), which shows maximum displacement at an

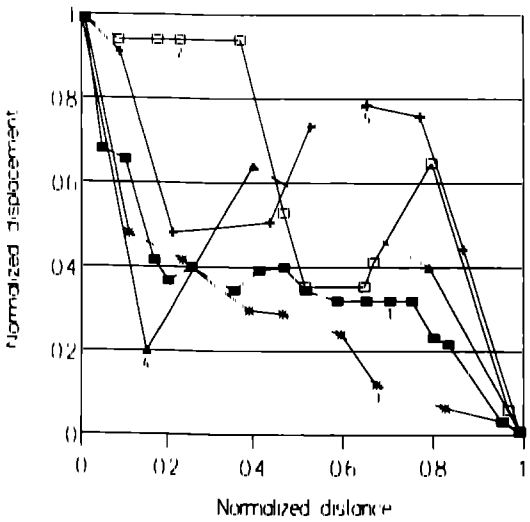

Fig. 12. D type D–X profiles. 1 = The southern end of the fault zone shown in Fig. 6(a) (segments G21, G22 and G23 added together), with depression below the C type profile caused by the contractional bend. 2 = Composite profile for the south of segments R10–R14, which form a large extensional offset/bend (Fig. 7a). 3 = Segment G21(S), with the D type profile caused by propagation beyond the contractional bend (Fig. 6a). 4 = Fault R6(N), which has a contractional bend and/or consists of linked segments. 5 = Segment R7(N), which appears to be composed of several small linked segments.

extensional offset, with displacement being transferred rapidly onto the adjacent segment.

CONCLUSIONS

Detailed mapping of small scale strike-slip fault zones at Raeberry and Gipsy Point, which have displacements of up to 1 m, has revealed several features which may be typical of other fault zones, including those with much greater displacements.

(1) The fault zones are composed of offset and linked segments.

(2) Lithologic variations, conjugate relationships, offsets, segment linkage and fault bends produce considerable variation in d–x graphs, with marked departures from the single event elastic model and from the cumulative slip model of Walsh & Watterson (1987).

(a) Lithologic variations, conjugate relationships, offsets and the linkage of segments of approximately the same size near their points of maximum displacements, all produce E type d–x profiles. These are convex up, *elevated* above the Walsh & Watterson (1987) cumulative slip profile because they have high displacement gradients at their tips. For such faults, the displacement increase is proportionally larger than the length as predicted by the Walsh & Watterson cumulative slip profile.

(b) Contractional bends and segment linkage points are often marked by displacement minima, which produces irregular D type profiles. These are partially concave up, *depressed* partially or completely below the Walsh & Watterson (1987) cumulative slip profile. Fault displacement minima occur where structures such as drag, ductile deformation and veins transfer displacement at bends and offsets. Total (brittle and ductile) deformation across linkages and bends may be approximately constant. Such faults have complex slip–propagation relationships.

(3) Four stages can be identified in the development of

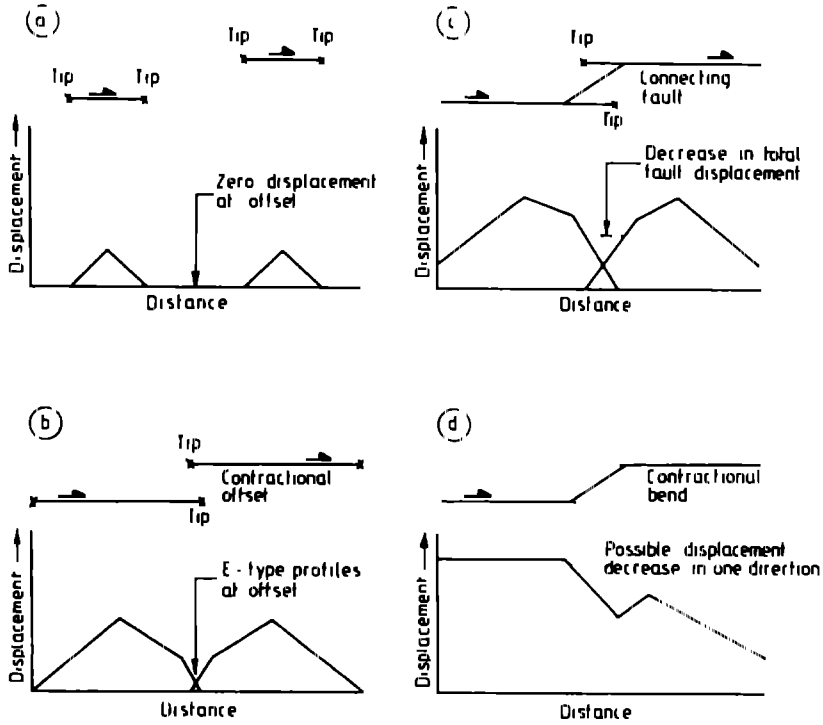

Fig. 13. Diagrams of stages in the development of a contractional bend, with corresponding displacement–distance graphs (cf. Peacock & Sanderson 1991, fig. 12). (a) Stage 1, offset, underlapping faults. (b) Stage 2, overlap of faults, with displacement transferred between the faults. (c) Stage 3, the offset faults are linked by connecting faults. (d) Stage 4, a contractional bend is produced, with normal drag causing a displacement decrease at the bend, with a possible displacement decrease in one direction.

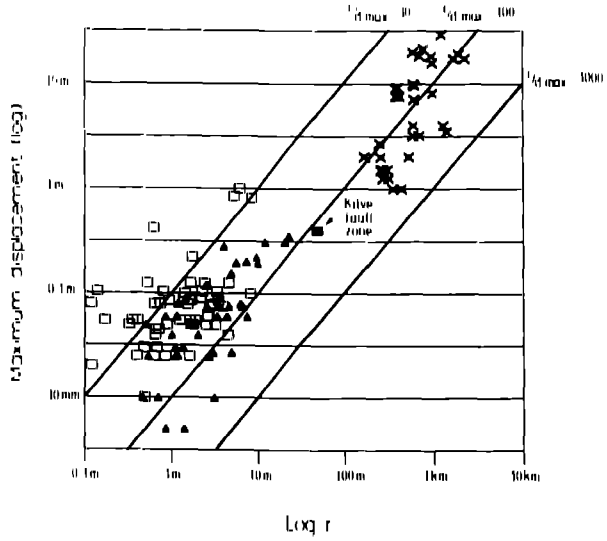

Fig. 14. Logarithmic (base 10) graph of r against d_{MAX}, where r = distance between the point of maximum displacement and the fault tip, and d_{MAX} = maximum displacement. Open squares = Raeberry and Gipsy Point, triangles = normal fault segment from Peacock & Sanderson (1991), filled square = normal fault zone from Peacock & Sanderson (1991), crosses = British coalfield normal fault data of Walsh & Watterson (1987). The Raeberry and Gipsy Point data have lower r/d_{MAX} ratios than the faults described by Peacock & Sanderson (1991) and the British coalfields faults.

displacement parallel offsets. Initially isolated faults (stage 1) can propagate towards each other so that interaction occurs (stage 2). Connecting fault(s) link the offset segments (stage 3) so that an extensional or contractional bend is produced (stage 4).

(4) Individual segments tend to have much lower r/d_{MAX} ratios than shown by British coalfield faults (Walsh & Watterson 1987), and by the normal fault segments of Peacock & Sanderson (1991). This may be because measurements at Raeberry and Gipsy Point are made parallel to the displacement direction and normal to anisotropy, with displacement gradients being higher in this direction.

Acknowledgements—I am grateful to M. T. Swanson, S. H. Treagus and an anonymous reviewer for their helpful comments. I am indebted to D. J. Sanderson, who supervised the post graduate research studentship, which was financed by the Natural Environment Research Council. The diagrams were produced with the help of P. Durnford. This paper is dedicated to Gordon C. Peacock.

REFERENCES

Barnes, R. P., Lintern, B. C. & Stone, P. 1989. Timing and regional implications of deformation in the Southern Uplands of Scotland. *J. geol. Soc. Lond.* **146**, 905–908.

Barnett, J. A. M., Mortimer, J., Rippon, J. H., Walsh, J. J. & Watterson, J. 1987. Displacement geometry in the volume containing a single normal fault. *Bull. Am. Ass. Petrol. Geol.* **71**, 925–937.

Ellis, M. A. & Dunlap, W. J. 1988. Displacement variation along thrust faults: implications for the development of large faults. *J. Struct. Geol.* **10**, 183–192.

Engelder, T. 1987. Joints and shear fractures in rock. In: *Fracture Mechanics of Rock* (edited by Atkinson, B. K.). Academic Press, New York, 27–69.

Granier, T. 1985. Origin, damping, and pattern of development of faults in granite. *Tectonics*, **4**, 721–737.

Horsfield, W. T. 1980. Contemporaneous movement along crossing conjugate normal faults. *J. Struct. Geol.* **2**, 305–310.

Hutton, D. H. W. & Murphy, F. C. 1987. The Silurian of the Southern Uplands and Ireland as a successor basin to the end Ordovician closure of Iapetus. *J. geol. Soc. Lond.* **144**, 765–772.

Kemp, A. E. S. 1986. Tectonostratigraphy of the Southern Belt of the Southern Uplands. *Scott. J. Geol.* **22**, 241–256.

Kemp, A. E. S. 1987. Tectonic development of the Southern Belt of the Southern uplands accretionary complex. *J. geol. Soc. Lond.* **144**, 827–838.

King, G. C. P. 1983. The accommodation of large strains in the upper lithosphere of the earth and other solids by self similar fault systems: the geometric origin of b value. *Pure Appl. Geophys.* **121**, 761–1091.

King, G. C. P. 1986. Speculations on the geometry of the initiation and termination processes of earthquake rupture and its relation to morphology and geological structure. *Pure & Appl. Geophys.* **124**, 567–585.

Leggett, J. K. 1987. The Southern Uplands as an accretionary prism: the importance of analogues in reconstructing palaeogeography. *J. geol. Soc. Lond.* **144**, 737–752.

Leggett, J. K., McKerrow, W. S. & Eales, M. H. 1979. The Southern Uplands of Scotland: a Lower Palaeozoic accretionary prism. *J. geol. Soc. Lond.* **136**, 755–770.

McCurry, J. A. & Anderson, T. B. 1989. Landward vergence in the lower Palaeozoic Southern Uplands Down Longford terrane, British Isles. *Geology* **17**, 630–633.

McKerrow, W. S. 1987. The Southern Uplands controversy. *J. geol. Soc. Lond.* **144**, 735–736.

McKerrow, W. S., Leggett, J. K. & Eales, M. H. 1977. Imbricate thrust model of the Southern Uplands of Scotland. *Nature* **267**, 237–239.

Muraoka, H. & Kamata, H. 1983. Displacement distribution along minor fault traces. *J. Struct. Geol.* **5**, 483–495.

Murphy, F. C. & Hutton, D. H. W. 1986. Is the Southern Uplands of Scotland really an accretionary prism? *Geology* **14**, 354–357.

Needham, D. T. & Knipe, R. J. 1986. Accretion and collision related deformation in the Southern Uplands accretionary wedge, southwestern Scotland. *Geology* **14**, 303–306.

Peacock, D. C. P. & Sanderson, D. J. 1991. Displacements, segment linkage and relay ramps in normal fault zones. *J. Struct. Geol.* **13**, 721–733.

Pollard, D. D. & Segall, P. 1987. Theoretical displacements and stresses near fractures in rock: with applications to faults, joints, veins, dikes, and solution surfaces. In: *Fracture Mechanics of Rock* (edited by Atkinson, B. K.). Academic Press, New York, 277–349.

Ramsay, J. G. & Huber, M. I. 1987. *The Techniques of Modern Structural Geology, Volume 2: Folds and Fractures*. Academic Press, London.

Stone, P., Floyd, J. D., Barnes, R. P. & Lintern, B. C. 1987. A sequential back arc and foreland basin thrust duplex model for the Southern Uplands of Scotland. *J. geol. Soc. Lond.* **144**, 753–764.

Swanson, M. T. 1989. Sidewall ripouts in strike slip faults. *J. Struct. Geol.* **11**, 933–948.

Swanson, M. T. 1990. Extensional duplexing in the York Cliffs strike slip fault system, southern coastal Maine. *J. Struct. Geol.* **12**, 499–512.

Walsh, J. J. & Watterson, J. 1987. Distributions of cumulative displacement and seismic slip on a single normal fault. *J. Struct. Geol.*, **9**, 1039–1046.

Walsh, J. J. & Watterson, J. 1989. Displacement gradients on fault surfaces. *J. Struct. Geol.* **11**, 307–316.

Wilcox, R. E., Harding, T. P. & Seely, D. R. 1973. Basic wrench tectonics. *Bull. Am. Ass. Petrol. Geol.* **57**, 74–96.

Williams, G. & Chapman, T. 1983. Strains developed in the hanging walls of thrusts due to their slip/propagation rate: a dislocation model. *J. Struct. Geol.* **5**, 563–571.

Woodcock, N. H. & Fischer, M. 1986. Strike slip duplexes. *J. Struct. Geol.* **8**, 725–735.